Field-induced superconducting phase in superconductor–normal metal and superconductor-superconductor bilayers

X. Montiel and A. I. Buzdin*

Condensed Matter Theory Group, LOMA, UMR 5798, Université Bordeaux 1, F-33405 Talence, France

(Received 6 April 2011; published 9 August 2011)

We study the proximity effect in a superconductor (S)–normal metal (N) bilayer system under in-plane magnetic field and demonstrate that a compensation between the Zeeman effect and the energy splitting between bonding and antibonding levels may lead to a magnetic-field-induced superconducting phase well above the standard paramagnetic limit. It occurs that the nonuniform Fulde-Ferrell-Larkin-Ovchinikov superconducting state also exists in the field-induced phase. The presence of the impurity scattering shrinks the region of field-induced superconductivity existence in S-N and S-S bilayers.

DOI: 10.1103/PhysRevB.84.054518 PACS number(s): 74.45.+c, 74.62.En, 74.78.−w

I. INTRODUCTION

Quasi-two-dimensional superconductors have been studied for fifty years. A strong upper critical magnetic field (H_{c2}) anisotropy was observed for the first time in intercalated layered crystals of dichalcogenides of transition metals.[1] In these compounds, H_{c2} is higher for the in-plane orientation (a-b plane) than in the perpendicular one (c axis). Moreover, this H_{c2} anisotropy was observed in intercalated graphite superconductors [in C_8K (Refs. 2 and 3), in C_6Ca (Refs. 4 and 5), and in C_6Yb (Ref. 5)], in organic superconductors,[6] in high superconducting critical temperature (high T_c) cuprate superconductors,[7–10] and also in superconducting-superconducting (S-S′) $YBa_2Cu_3O_7/DyBa_2Cu_3O_7$ and superconducting-insulating (S-I) $(YBa_2Cu_3O_7)_n/(Pr\,Ba_2Cu_3O_7)_m$ artificial superlattices.[11,12] High-T_c cuprate superconductors have a layered crystal structure[13] and a strong electron anisotropy.[7,13–17] The superconducting coherence length along the c axis ξ_c is smaller than the interlayer distance d. Consequently, high-T_c cuprate superconductors can be considered as natural superlattices. In high-T_c cuprate superconducting compounds, superconductivity exists in CuO_2 atomic planes which are sandwiched by non-superconducting atomic planes.[13,18]

The Ginzburg-Landau model [in the weak-anisotropy limit ($\xi_c \lesssim d$)][19] and the Lawrence-Doniach model [in the strong-anisotropy limit ($\xi_c \ll d$)][20] give the description of the H_{c2} anisotropic properties in layered superconductors near T_c. This H_{c2} anisotropy in superconducting multilayers can also be described microscopically by the standard Bardeen-Cooper-Schrieffer (BCS) theory and the tunneling Hamiltonian theory. Using this method, we obtain the (H_{c2},T) phase diagram of layered superconducting systems.

Some of high-T_c cuprate superconductors can be considered as a stack of S-N, S-S′,[21] or S-F[22] weakly coupled bilayers. The S-N, S-S′, or S-F bilayer constitutes the elemental unit cell of the multilayer. The properties of the S-N, S-S′, or S-F bilayers qualitatively differ from single S, N, or F layers. Consequently, the properties of multilayers based on a single-layer elemental unit cell may be qualitatively different from the properties of multilayers based on a bilayer elemental unit cell. We show in this paper that the (H,T) phase diagram, with in-plane magnetic field, of S-N and S-S′ bilayers may reveal a magnetic-field-induced superconducting phase.

The case of S-F multilayers has been studied in Refs. 22–25. In the S-S bilayer, Buzdin *et al.* have demonstrated[26,27] the possibility to overcome the paramagnetic limit at low temperature for a high in-plane critical magnetic field. The field-induced superconducting phase may appear at high magnetic field if the interlayer coupling energy t is higher than T_c. Moreover, in this phase, the adjacent S layers have opposite signs of the order parameter (this is the so-called π state[22]). In this case, the Zeeman effect is compensated by the bonding-antibonding degeneracy lift produced by the hybridization between the two S layers (see Fig. 1). The Cooper pairs in the π state are more stable at high magnetic field than the 0 state. The 0 state occurs when the adjacent S layers support the same signs of the order parameter. A somewhat similar idea in the context of two-band superconductivity was introduced by Kulic and Hofmann.[28] In this paper, we show that in a S-N bilayer at high in-plane magnetic field H (see Fig. 2), at low temperature and strong enough coupling $t > T_{c0}$ between the two planes, the paramagnetic limit is also enhanced above the usual Fulde-Ferrell-Larkin-Ovchinikov (FFLO)[29,30] limit and a field-induced superconducting phase may appear at high magnetic field. The adjacent N layer certainly decreases the transition temperature but, on the other hand, it could increase substantially the parallel critical field at $T = 0$ K. The corresponding mechanism is qualitatively the same as in the S-S bilayer. However, in S-S bilayer this regime corresponds to the transition from the 0 state into the π state, while for S-N bilayer such π phase cannot exist. We study also the influence of the impurity scattering on the (H,T) phase diagram of S-N and S-S bilayers.

The outline of the paper is as following. In Sec. II, we present the model of a multilayer system and give the exact solutions of the Eilenberger equations for S-N systems. In Sec. III, we study the influence of the transfer integral on the superconducting critical temperature and we present the (H,T_c) and (H,t) phase diagrams. In Sec. IV, we investigate the influence of impurities on the superconducting critical temperature and (H,T_c) and (H,t) phase diagrams. In Sec. V, we study the influence of impurities on the S-S bilayer (H,T_c) phase diagram.

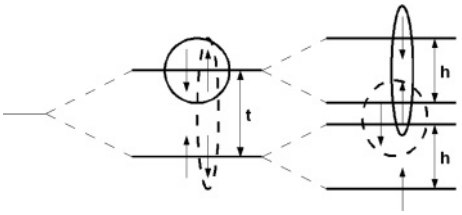

FIG. 1. Mechanism of compensation of the Zeeman effect by the degeneracy lifting between the bonding and antibonding states.

II. MODEL OF AN ATOMIC THICKNESS S-N BILAYER

We start with a noninteracting model (see for example Refs. 22 and 31) of layered systems with alternating superconducting and normal metal layers. The electron motion is described in the N and S layers by the spin-dependent energy spectra $\xi_{n,\sigma}(\mathbf{k})$ and $\xi_{s,\sigma}(\mathbf{k})$, respectively. The parameters that characterize the systems are the transfer energy between the N and S layers t and the Cooper pairing constant λ, which is assumed to be nonzero in S layers only. The Zeeman energy splitting, due to in-plane magnetic field H, is written as $h = \mu_B H$ where μ_B is the Bohr magneton.

The two mechanisms destroying superconductivity under a magnetic field are the orbital and the paramagnetic effects.[32,33] Usually it is the orbital effect that is more restrictive. However, in systems with a large effective mass of electrons[34,35] or in low-dimensional compounds, such as quasi-one-dimensional or layered superconductors under in-plane magnetic field,[36] the orbital magnetism is weakened and it is the paramagnetic effect that is responsible for superconductivity destruction.

The Chandrasekhar-Clogston paramagnetic limit[37,38] is achieved when the polarization energy of the normal electron gas, $\chi_n H^2/2$, equals the superconducting condensation energy $N(0)\Delta_0^2/2$, where $N(0)$ is the density of state of the normal electron gas, χ_n is its spin susceptibility, and $\Delta_0 = 1.76T_c$ is the zero-temperature superconducting gap. This criterion gives the exchange field $h_p(T=0) = \Delta_0/\sqrt{2}$ where the superconductor should undergo a first-order transition to the normal state. Larkin and Ovchinikov[29] and Fulde and Ferrell[30] (FFLO) predicted the existence of a nonuniform superconducting state with slightly higher critical field $h^{3D}_{\mathrm{FFLO}}(T=0) = 0.755\Delta_0 > h_p(T=0)$. For quasi-2D superconductors the critical field of the FFLO state is even higher, namely $h^{2D}_{\mathrm{FFLO}}(T=0) = \Delta_0$,[39] while in quasi-one-dimensional systems there is no paramagnetic limit at all.[40] We focus on the 2D case for which a generic temperature magnetic field phase diagram has been established.[39]

We consider the case when the coupling between the layers is realized via the transfer energy t. In the whole paper, we assume $t \ll E_F$ where E_F is the Fermi energy and then Cooper

FIG. 2. (Color online) A superconducting (S)–normal metal (N) bilayer with in-plane magnetic field H.

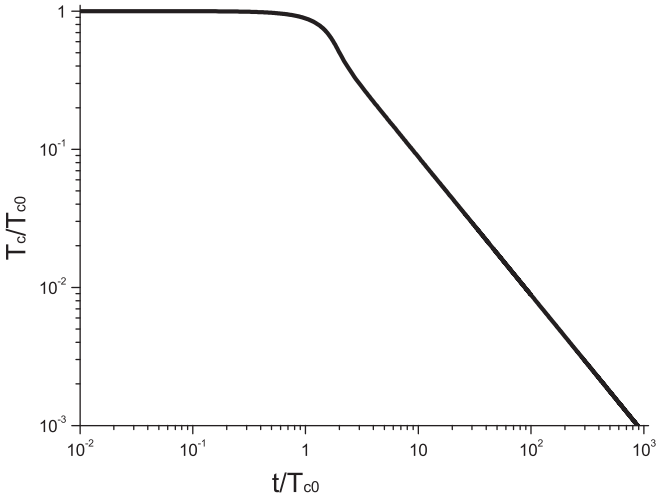

FIG. 3. Graph of T_c/T_{c0} as a function of t/T_{c0} (solid line). For $t \gg T_{c0}$, the critical temperature of the superconductor decreases to zero.

pairs are localized within each plane. The layers are coupled together by the coupling Hamiltonian

$$\hat{H}_t = t \sum_{j,\sigma,\mathbf{k}} [\psi^+_{j+1,\sigma}(\mathbf{k})\psi_{j,\sigma}(\mathbf{k}) + \psi^+_{j,\sigma}(\mathbf{k})\psi_{j+1,\sigma}(\mathbf{k}) + \mathrm{H.c.}], \tag{1}$$

where $\psi^+_{j,\sigma}(\mathbf{k})$ [resp. $\psi_{j,\sigma}(\mathbf{k})$] is the creation (resp. annihilation) operator of an electron with spin σ and momentum $\mathbf{k}$ in the jth layer. In this paper, we study the S-N and S-S bilayers. In the S-N system, the superconducting layer has the index $j = 0$ and the normal metal $j = 1$. In the S-S bilayer, the superconducting layers are indexed $j = 0$ and $j = 1$. The Hamiltonian of the system can be written as

$$\hat{H} = \hat{H}_0 + \hat{H}_{\mathrm{BCS}} + \hat{H}_t, \tag{2}$$

where H_0 is the kinetic and Zeeman Hamiltonian, H_t the tunneling Hamiltonian, and H_{BCS} the BCS Hamiltionian. For the jth layer, the kinetic and Zeeman parts of the Hamiltonian are written as

$$\hat{H}_0 = \sum_{\sigma,\mathbf{k}} [\xi_{j,\sigma}(\mathbf{k},h_j)\psi^+_{j,\sigma}(\mathbf{k})\psi_{j,\sigma}(\mathbf{k})]. \tag{3}$$

The Zeeman effect manifests itself in breaking the spin degeneracy of the electronic energy levels according to

$$\xi_{j,\sigma}(\mathbf{k},h_j) = \xi_j(\mathbf{k}) - \sigma h_j, \tag{4}$$

where $\xi_j(\mathbf{k}) = \mathbf{k}^2/2m - E_F$; i.e., for simplicity we choose the same electron spectrum in both layers.

The field h_j in the jth layer is assumed to be the same in both layers ($h_0 = h_1 = h$). We suppose an s-wave singlet

superconductivity coupling which is treated in $H_{\rm BCS}$ within a mean-field approximation[41]

$$\hat{H}_{\rm BCS} = \sum_{j,\mathbf{k}} [\Delta_j^*(\mathbf{q})\psi_{j,\downarrow}^+(\mathbf{k})\psi_{j,\uparrow}^+(-\mathbf{k}) + \Delta_j(\mathbf{q})\psi_{j,\uparrow}(\mathbf{k})\psi_{j,\downarrow}(-\mathbf{k})] + \frac{1}{|\lambda|}\int \mathbf{d}^2\mathbf{r}\Delta_j^2(\mathbf{r}), \quad (5)$$

where $\boldsymbol{r}$ is the two-dimensional coordinate within each layer and λ the electron-electron coupling constant in the S layer only. The superconducting order parameter Δ_j is nonzero only in the S layers as the coupling constant is 0 in the N layer. In order to investigate the occurrence of modulated superconducting phase (FFLO), we choose the superconducting order parameter in the form

$$\Delta(\mathbf{r}) = \Delta e^{i\mathbf{q}\cdot\mathbf{r}},$$

where $\mathbf{q}$ is the FFLO modulation wave vector. Using Gorkov's formalism, we introduce the normal G and anomalous $\widetilde{F}$ Green's functions[41]:

$$G_{j,l}(\mathbf{k},\mathbf{k}') = -\langle T_\tau(\psi_{\uparrow,j}(\mathbf{k})\psi_{\uparrow,l}^+(\mathbf{k}'))\rangle = \delta(\mathbf{k}-\mathbf{k}'+\mathbf{q})G_{j,l}(\mathbf{k}), \quad (6)$$

$$F_{j,l}^+(\mathbf{k},\mathbf{k}') = \langle T_\tau(\psi_{\downarrow,j}^+(\mathbf{k})\psi_{\uparrow,l}^+(\mathbf{k}'))\rangle = \delta(\mathbf{k}+\mathbf{k}')F_{j,l}^+(\mathbf{k}),$$

where the brackets mean statistical averaging over grand-canonical distribution, T_τ is the ordering operator in the Matsubara formalism,[41] and j and l are the layer's indexes. From the equation of motion,[41] the system of Green's functions equation is, in the Fourier representation in the S-N bilayer,

$$\begin{pmatrix} i\omega - \xi_{0,\uparrow}(\mathbf{k}+\mathbf{q}) & -t & \Delta_0 & 0 \\ -t & i\omega - \xi_{1,\uparrow}(\mathbf{k}+\mathbf{q}) & 0 & 0 \\ \Delta_0^* & 0 & i\omega + \xi_{0,\downarrow}(\mathbf{k}) & t \\ 0 & 0 & t & i\omega + \xi_{1,\downarrow}(\mathbf{k}) \end{pmatrix} \begin{pmatrix} G_{0,0}(\mathbf{k}+\mathbf{q}) \\ G_{1,0}(\mathbf{k}+\mathbf{q}) \\ F_{0,0}^+(\omega,\mathbf{k}) \\ F_{1,0}^+(\omega,\mathbf{k}) \end{pmatrix} = \begin{pmatrix} 1 \\ 0 \\ 0 \\ 0 \end{pmatrix},$$

where $\omega = (2n+1)\pi T$ are the fermionic Matsubara frequencies. In quasi-2D superconductors, the maximal modulus of the FFLO wave vector is of the order of $(\xi_0)^{-1}$, ξ_0 being the typical superconducting coherence length. Since $\xi_0 \gg \frac{1}{k_F}$, which is of the order of the interatomic distance, with a good approximation we can consider $\xi_{j,\uparrow}(\mathbf{k}+\mathbf{q}) = \xi(\mathbf{k}) - h + \mathbf{v}_F\cdot\mathbf{q}$, where $\mathbf{v}_F$ is the Fermi velocity vector in the plane. The anomalous Green's function in the S layer can be written as

$$F_{0,0}^+ = \frac{-\Delta_0^* A}{-\alpha_0 A - \beta t^2 + t^4},$$

where $A = [i\omega - \xi(\mathbf{k}) + h - v_F q][i\omega + \xi(\mathbf{k}) + h]$, $\alpha_0 = |\Delta_0|^2 - [i\omega - \xi(\mathbf{k}) + h - v_F q][i\omega + \xi(\mathbf{k}) + h]$, and $\beta = [i\omega - \xi(\mathbf{k}) + h - v_F q]^2 + [i\omega + \xi(\mathbf{k}) + h]^2$. The superconducting order parameter in the 0th superconducting layer satisfies the self-consistency equation

$$\Delta_0^* = |\lambda| T \sum_{\omega>0}\sum_{\mathbf{k}} F_{0,0}^+ = |\lambda| T \sum_{\omega}\int_{-\infty}^{+\infty} F_{0,0}^+ d\xi. \quad (7)$$

To describe the FFLO modulated phase and the influence of the impurities it is more convenient to use the quasi-classical Eilenberger formalism. Moreover, we include the FFLO modulation phase and nonmagnetic impurities. Applying Eilenberger's method[42] for a layered system[43] with Hamiltonian (2), the system of equations of Green's functions can be written as

$$\begin{pmatrix} \widetilde{\omega} - i\mathbf{v}_F\cdot\mathbf{q} & -i\frac{t}{2} & 0 & i\frac{t}{2} \\ -i\frac{t}{2} & \widetilde{\omega} - i\mathbf{v}_F\cdot\mathbf{q} & i\frac{t}{2} & 0 \\ 0 & i\frac{t}{2} & \widetilde{\omega} - i\mathbf{v}_F\cdot\mathbf{q} & -i\frac{t}{2} \\ i\frac{t}{2} & 0 & -i\frac{t}{2} & \widetilde{\omega} - i\mathbf{v}_F\cdot\mathbf{q} \end{pmatrix} \begin{pmatrix} f_{0,0}^+ \\ f_{1,0}^+ \\ f_{1,1}^+ \\ f_{0,1}^+ \end{pmatrix} = \begin{pmatrix} \Delta_0^* + \frac{\langle f_{0,0}^+(\omega,\mathbf{q})\rangle_\phi}{2\tau} \\ 0 \\ 0 \\ 0 \end{pmatrix}, \quad (8)$$

where $\widetilde{\omega} = \omega + ih + (1/2\tau)$, $f_{j,l}^+(\omega,\mathbf{q}) = \frac{1}{i\pi}\int_{-\infty}^{+\infty} d\xi F_{j,l}^+(\omega,\xi,\mathbf{q})d\xi$ is the anomalous Green's function in the Eilenberger formalism, and τ is the electron mean-free path time. We write $\mathbf{v}_F\cdot\mathbf{q} = v_F q\cos(\phi)$, where ϕ is the polar angle $(\mathbf{v}_F,\mathbf{q})$, and $\langle\rangle_\phi$ is the average over ϕ. We assume an in-plane scattering on impurities and the absence of spin flip during the electron-impurity interaction. To consider the presence of impurities we substitute ω by $\omega + 1/2\tau$ and Δ_j^* by $\Delta_j^* + \langle f_{j,j}^+(\omega,\mathbf{q})\rangle_\phi/2\tau$; see for example Ref. 43.

Solving the Eilenberger equation (8) yields the Eilenberger Green's function for the S layer labeled $j = 0$:

$$f_{0,0}^+ = \frac{\Delta_0^*}{2\left\{1 - \frac{(1/2\tau)[\Omega_1\Omega_3 + \Omega_2\Omega_3 + 2\Omega_1\Omega_2]}{4\Omega_1\Omega_2\Omega_3}\right\}}\left\{\frac{1}{\omega_3} + \frac{1}{2\omega_1} + \frac{1}{2\omega_2}\right\}, \quad (9)$$

where we pose $\Omega_{1,2}^2 = \widetilde{\omega}_{\pm}^2 + v^2q^2$, $\Omega_3^2 = \widetilde{\omega}^2 + v^2q^2$ with $\widetilde{\omega} = \omega + ih + (1/2\tau)$, $\widetilde{\omega}_{\pm} = \omega + ih + (1/2\tau) \pm it$, $\omega_3 = \widetilde{\omega} - iv_F\, q\, \cos(\phi)$ with $\omega_{1,2} = \omega_3 \pm it = \widetilde{\omega}_{\pm} - iv_F\, q\, \cos(\phi)$. The averaged solution on the ϕ angle of (9) can be written

$$\langle f_{0,0}^{+}\rangle_{\phi} = \frac{\Delta_0^*}{2\left\{1 - \frac{(1/2\tau)[\Omega_1\Omega_3 + \Omega_2\Omega_3 + 2\Omega_1\Omega_2]}{4\Omega_1\Omega_2\Omega_3}\right\}} \times \left\{\frac{1}{\Omega_3} + \frac{1}{2\Omega_1} + \frac{1}{2\Omega_2}\right\}, \tag{10}$$

where $\langle\rangle_{\phi}$ is the average on the ϕ angle. Close to the superconducting critical temperature of the second-order phase transition, the self-consistency (7) can be written[33]

$$\ln\left(\frac{T_c}{T_{c_0}}\right) = \mathrm{Re}\left(\sum_{\omega>0}\left(\left\langle \widetilde{f}_{\downarrow\uparrow}^{0,0}(\omega,q)\right\rangle_{\phi} - \frac{\pi}{\omega}\right)\right), \tag{11}$$

where T_c is the critical temperature of the superconducting layer in the S-N bilayer and $T_{c0} = \frac{2\gamma\omega_D}{\pi}\exp(-\frac{2\pi^2}{|\lambda|mk_F})$ is the critical temperature of an isolated superconducting layer with m the electron's mass, k_F the Fermi impulsion, $\gamma = 0.577215$ the Euler's constant, and ω_D the Debye frequency.

At zero temperature, close to the critical magnetic field of the second-order phase h_0, the order parameters Δ_j are also small and the self-consistency (7) can be written

$$\ln\left(\frac{h}{h_0}\right) = \frac{2T_c}{\pi}\int_0^{+\infty}\mathrm{Re}\left(\left\langle \widetilde{f}_{\downarrow\uparrow}^{0,0}(\omega,q)\right\rangle_{\phi} - \frac{\pi}{\omega + ih_0}\right)d\omega. \tag{12}$$

III. PROXIMITY EFFECT IN S-N BILAYER

In this section, we investigate the superconducting phase in the S-N bilayer in the clean limit ($\tau \to \infty$). We study the superconducting critical temperature as a function of the interlayer coupling. We obtain the critical magnetic field of second-order superconducting to normal metal phase transition as a function of the temperature and the interlayer coupling. Studies of the influence of the impurities on the S-N bilayer and the S-S bilayer are respectively proposed in Secs. IV and V.

A. Critical temperature

We study first the influence of the proximity effect on the superconducting critical temperature T_c of the S layer when no magnetic field is applied ($h = q = 0$) in the clean limit ($\tau \to \infty$). Then (10) becomes

$$f_{0,0}^{+} = \frac{\Delta^*(t^2 + 2\omega^2)}{2\omega(t^2 + \omega^2)}; \tag{13}$$

thus the self-consistency equation can be written

$$\ln\left(\frac{T_c}{T_{c0}}\right) = -\frac{1}{4}\left[2\gamma + 4\ln 2 + \Psi\left(\frac{1}{2} - \frac{it}{2\pi T_c}\right) + \Psi\left(\frac{1}{2} + \frac{it}{2\pi T_c}\right)\right],$$

where $\Psi(x)$ is the digamma function. As seen in Fig. 3, the superconducting critical temperature decreases with the increase of the proximity effect. At low transfer energy $t \ll T_c$, the superconducting critical temperature varies as $\frac{T_c}{T_{c0}} = 1 - \frac{7}{8}\frac{\zeta(3)}{\pi^2}(\frac{t}{T_{c0}})^2$. In the case of low interlayer coupling, the superconducting critical temperature reveals a quadratic decrease with the transfer energy. The superconducting state is not qualitatively influenced by the normal metal layer and can be considered as a single superconducting layer.

At strong coupling between S and N layers at $t \gg T_c$ (but in the limit $t \ll \omega_D$), the superconducting temperature varies as $\frac{T_c}{T_{c0}} = \frac{\pi e^{-\gamma}}{2}\frac{T_{c0}}{t}$. The critical temperature decreases with the tunneling transfer as more and more Cooper pairs leak into the N layer. The superconducting properties in the N and S layers are practically the same and the bilayer can be considered as an equivalent single S layer with an effective coupling constant $\widetilde{\lambda}$ where $\widetilde{\lambda} < \lambda$. In the case where $t \gg \omega_D$, the S-N bilayer can be considered as a single superconducting layer S with $\widetilde{\lambda} = \frac{|\lambda|}{2}$ as predicted in Ref. 31.

B. Phase diagram of the S-N bilayer

We study the (h,T) and (h,t) phase diagram of the S-N bilayer in the clean case and in the presence of nonmagnetic impurities. In a two-dimensional S monolayer, we can define three critical magnetic fields at zero temperature. $h_0 = \Delta_0/2$ is the critical magnetic field for a second-order phase transition. $h^I = \Delta_0/\sqrt{2}$ is the critical magnetic field for a first-order phase transition defined by Clogston-Chandrasekar.[37,38] $h^{\mathrm{FFLO}} = \Delta_0$ is the critical magnetic field in the presence of FFLO modulations. One can see that $h^{\mathrm{FFLO}} > h^I > h_0$. In a clean S monolayer with an applied in-plane magnetic field, the critical field is h^{FFLO} (Ref. 33).

In this case, the Eilenberger anomalous Green's function (9) becomes for arbitrary interlayer coupling t

$$f^{+}(0,0) = \frac{\Delta^*}{2}\left[\frac{1}{\omega + ih + i\vec{v}_F\cdot\vec{q}} + \frac{1}{2(\omega - it + ih + i\vec{v}_F\cdot\vec{q})} + \frac{1}{2(\omega + it + ih + i\vec{v}_F\cdot\vec{q})}\right], \tag{14}$$

where we note the appearance of three energy scales $E_3 = h + \vec{v}_F\cdot\vec{q}$ and $E_{1,2} = h \pm t + \vec{v}_F\cdot\vec{q}$.

1. (h,t) phase diagram at zero temperature

From (14) and the self-consistency equation (12), the critical magnetic field h_c is shown to satisfy

$$\left|h_c - t + \sqrt{|(h_c - t)^2 - (q\,v_F)^2|}\right| \times \left|h_c + t + \sqrt{|(h_c + t)^2 - (q\,v_F)^2|}\right| \times \left|h_c + \sqrt{\left|h_c^2 - (q\,v_F)^2\right|}\right|^2 = h_0^4, \tag{15}$$

where one must find the value of q that maximizes the critical field h_c. If the field-induced phase is assumed to be uniform in each of the planes, namely if $q = 0$, Eq. (15) merely reduces to

$$|h_c|^2\,|h_c - t|\,|h_c + t| = h_0^4. \tag{16}$$

The number of solutions with physical meaning of Eq. (16) differs with the value of t (see Fig. 4). We define the critical interlayer coupling $t_c = \sqrt{2}h_0 = 1.2473T_{c0}$ that determines the number of physical solutions.

If $t < t_c$, Eq. (16) has only one solution. The critical magnetic field at zero temperature can be written $h_{c1} = \frac{1}{2}[2t^2 + 2(t^4 + 4h_0^4)^{1/2}]^{1/2}$. In the limit $t \ll T_{c0}$, the solution can be written $h_{c1} = \frac{\Delta_0}{2}(1 + \frac{t^2}{\Delta_0^2})$. We note that the critical magnetic field at $T = 0$ K in the S-N bilayer increases with the interlayer coupling t.

In the case $t > t_c$, Eq. (16) has three solutions with physical meaning. The first solution is h_{c1}. The second and the third solutions are $h_{c2} = \frac{1}{2}[2t^2 + 2(t^4 - 4h_0^4)^{1/2}]^{1/2}$ and $h_{c3} = \frac{1}{2}[2t^2 - 2(t^4 - 4h_0^4)^{1/2}]^{1/2}$, respectively. In the limit $t \gg T_{c0}$, the three solutions can be written as $h_{c1,2} = t \pm \Delta_0^4/32t^3$ and $h_{c3} = \Delta_0^2/4t$. In the limit $t \gg T_{c0}$, T_c is of the order of T_{c0}^2/t and then h_{c3} is of the order of T_c. Consequently, h_{c3} defines the lowest critical magnetic field.

For $t = t_c$ the critical fields h_{c2} and h_{c3} coincide.

In the case of high interlayer coupling $t > t_c$, a field-induced superconducting phase appears at high magnetic field. This phase exists between the two magnetic fields $h_{c1,2} = t \pm \Delta_0^4/32t^3$. Thus, the new zero-temperature paramagnetic limit $h_{c1} = t + \Delta(0)^4/32t^3$ may be tuned far above the usual one $h^{\mathrm{FFLO}} = \Delta_0$ merely by increasing the interlayer coupling.

Thorough analysis of Eq. (15) shows that the upper critical field is even increased by an in-plane modulation (see Fig. 5).

The FFLO paramagnetic limit of the S-N bilayer also depends on the interlayer coupling t as seen in Fig. 5. The field-induced superconducting phase is observable at $T = 0$ K only when h_{c2} and h_{c3} are distinguishable. In the presence of FFLO modulation, the critical magnetic field at zero temperature h_{c2}^{FFLO} and h_{c3}^{FFLO} are separated in the case $t \gtrsim 1.5T_{c0}$. Below this value, the usual superconducting (h,T) phase diagram may be strongly deformed (see Fig. 6).

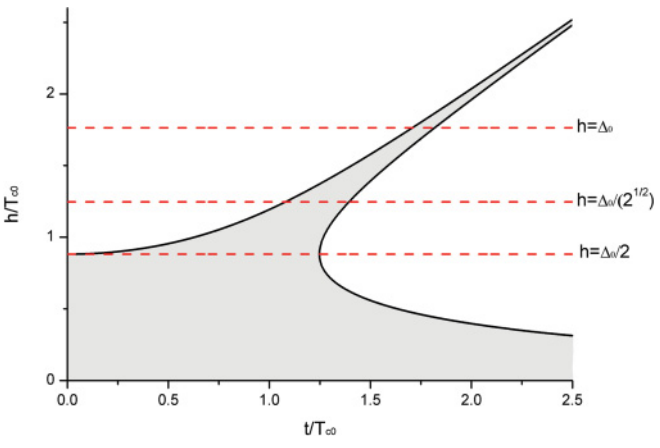

FIG. 4. (Color online) $(h/T_{c0}, t/T_{c0})$ diagram for the S-N bilayer in the clean limit $(\tau \to \infty)$ at $T = 0$ K (solid line). The uniform superconducting state is presented in gray. The line $h = \Delta_0/2$ presents the critical magnetic field for a second-order superconducting phase transition for a single superconducting layer. The line $h = \Delta_0$ corresponds the FFLO paramagnetic limit for a single superconducting layer. The line $h = \Delta_0/\sqrt{2}$ represents the first-order paramagnetic limit for a single superconducting layer.

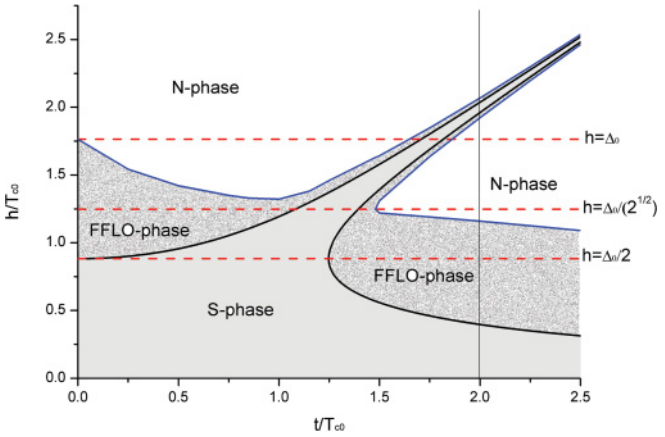

FIG. 5. (Color online) $(h/T_{c0}, t/T_{c0})$ diagram for the S-N bilayer in the clean limit $(\tau \to \infty)$ (solid line). The uniform superconducting state is presented in the gray region. The nonuniform superconducting (FFLO) phase in the S-N bilayer is presented in the dotted region. The line $h = \Delta_0/2$ presents the critical magnetic field for a second order superconducting phase transition for a single superconducting layer. The line $h = \Delta_0$ represents the FFLO paramagnetic limit for a single superconducting layer. The line $h = \Delta_0/\sqrt{2}$ represents the first-order paramagnetic limit for a single superconducting layer.

2. (h,T) *phase diagram*

In this section, we study the second-order (h,T) phase transition diagram taking into account FFLO modulation. The self-consistency Eq. (11) is

$$\ln\left(\frac{T_{c0}}{T_c}\right) = 2T_c \int_0^{2\pi} \frac{d\phi}{2\pi} \mathrm{Re}\left[\gamma + 2\ln(2) + \frac{1}{4} \times \Psi\left(\frac{1}{2} + \frac{i(h + v_F q\ \cos(\phi))}{2\pi T}\right)\right] + 2T_c \int_0^{2\pi} \frac{d\phi}{2\pi} \times \mathrm{Re}\left[\frac{1}{8}\Psi\left(\frac{1}{2} + \frac{i(h + t + v_F q\ \cos(\phi))}{\pi T}\right) + \frac{1}{8}\Psi\left(\frac{1}{2} + \frac{i(h - t + v_F q\ \cos(\phi))}{\pi T}\right)\right]. \quad (17)$$

This analysis in the general case can be performed only numerically on the basis of (17).

A magnetic-field-induced superconducting state appears at high magnetic field as we can see in Fig. 7 for $t = 2T_{c0}$ and in Fig. 8 for $t = 3T_{c0}$. For $h \simeq t$, the Zeeman effect that destroys the superconductivity is compensated by the bonding-antibonding states degeneracy created by the proximity effect between the S and the N layers (see Fig. 1). The lower and upper critical lines merge at field $h = t$ and the field-induced superconductivity is confined to temperature lower than $T_M = \pi e^{-\gamma} T_{c0}^2/(8t)$ in the limit $t \gg T_{c0}$. Therefore, the superconducting field-induced phase is confined to temperature lower than T_M. These results were obtained for relatively strong coupling. For lower coupling

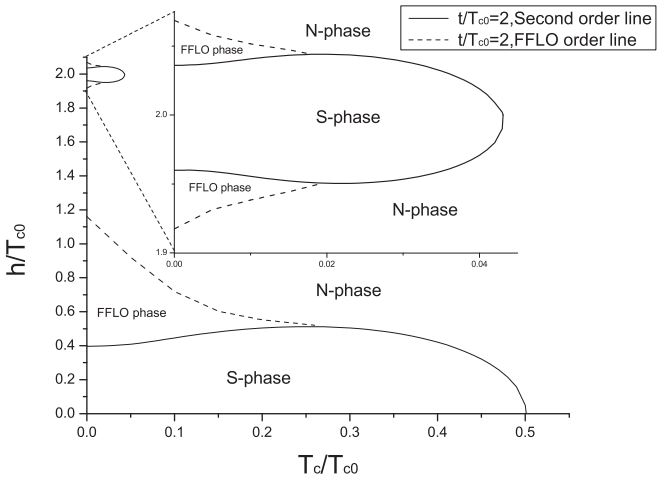

FIG. 6. $(h/T_{c0}, T_c/T_{c0})$ phase transition diagram calculated for $t = 1.35T_{c0}$ with the second-order transition line (solid line) and FFLO state to normal state transition line (dotted line). We see below $T_c \simeq 0.2T_{c0}$ that the transition line is deformed. The compensation between the Zeeman effect and the bonding and antibonding states becomes relevant at low temperature.

$(t \simeq T_{c0})$, the usual phase transition diagram is strongly deformed as shown in Fig. 6 and finally disappears for t smaller enough than T_{c0}. From an experimental point of view, one might choose a system with an intermediate coupling t small enough to settle the superconducting field-induced phase but large enough to separate reentrance and the usual S phase.

IV. EFFECT OF THE IMPURITIES ON THE FIELD-INDUCED SUPERCONDUCTING PHASE

In this section, we investigate phases with uniform superconductivity in the S layer. We study the superconducting critical temperature as a function of the interlayer coupling. We obtain the critical magnetic field of the second-order

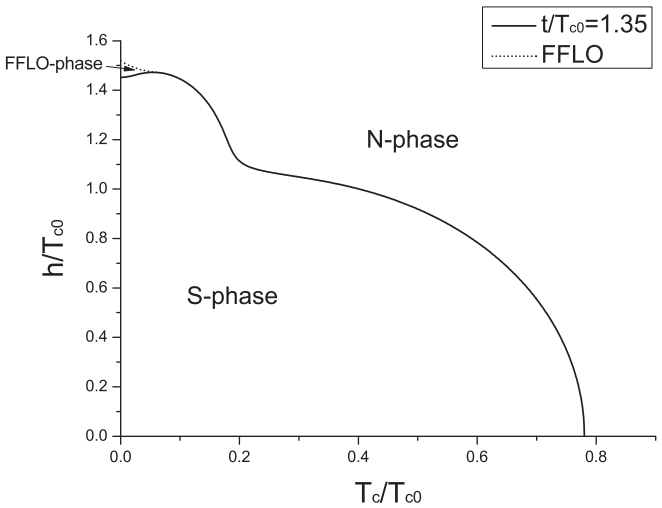

FIG. 7. $(h/T_{c0}, T_c/T_{c0})$ phase transition diagram calculated for $t = 2T_{c0}$ with the second-order transition line (solid line) and FFLO state to normal state transition line (dotted line). The inset presents a zoom of the superconducting reentrance phase around $h \simeq t \simeq 2T_{c0}$.

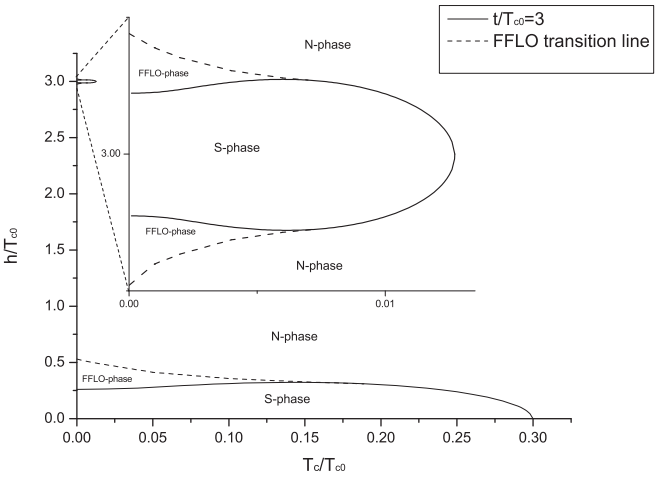

FIG. 8. $(h/T_{c0}, T_c/T_{c0})$ phase transition diagram calculated for $t = 3T_{c0}$ with the second-order transition line (solid line) and FFLO state to normal state transition line (dotted line). The inset presents a zoom of the superconducting reentrance phase around $h \simeq t \simeq 3T_{c0}$.

superconducting to normal metal phase transition as a function of the temperature and the interlayer coupling. Study of the influence of the impurities on the S-S bilayer is proposed in Sec. V.

A. Critical temperature

We start with the analysis of the influence of the impurities on the superconducting critical temperature. Then Eq. (10) can be written

$$f_{0,0}^{+} = \frac{\Delta^*\left(t^2 + 2\left(\omega + \frac{1}{2\tau}\right)^2\right)}{\left(2\omega + \frac{1}{2\tau}\right)t^2 + 2\omega\left(\omega + \frac{1}{2\tau}\right)^2} \tag{18}$$

in accordance with the model developed in Ref. 31. The self-consistency equation (11) in this case is written as

$$\ln\left(\frac{T_c}{T_{c0}}\right) = 2\pi T_c \sum_{\omega=0}^{\infty}\left(\frac{t^2 + 2\left(\omega + \frac{1}{2\tau}^2\right)}{\left(2\omega + \frac{1}{2\tau}\right)t^2 + 2\omega\left(\omega + \frac{1}{2\tau}\right)^2} - \frac{1}{\omega}\right). \tag{19}$$

In the case of weak proximity effect $(t \ll T_{c0})$, the decrease of the critical temperature is deduced from Eq. (19) and reads

$$\frac{T_c - T_{c0}}{T_{c0}} = \frac{\Delta T_c}{T_{c0}} = -\frac{1}{2}(\tau t)^2\left[\left(\frac{1}{2\tau T_{c0}}\right)\pi + 4\Psi\left(\frac{1}{2}\right) - 4\Psi\left(\frac{1}{2} + \frac{1}{4\tau T_{c0}\pi}\right)\right].$$

In the clean limit $(T_{c0} \gg t \gg \frac{1}{2\tau})$ the superconducting critical temperature varies as $\frac{T_c}{T_{c0}} = 1 - (\frac{7}{8}\frac{\zeta(3)}{\pi^2} - \frac{\pi}{192}\frac{1}{\tau T_{c0}})\frac{t^2}{T_{c0}^2}$, and the impurity scattering inside the N layer decreases the proximity effect. In the dirty regime $(T_{c0} \gg \frac{1}{2\tau} \gg t)$ the superconducting critical temperature varies as $\frac{T_c}{T_{c0}} = 1 - \frac{\pi}{2}\frac{\tau t^2}{T_{c0}}$. The presence of impurities enhanced the superconducting state and T_c

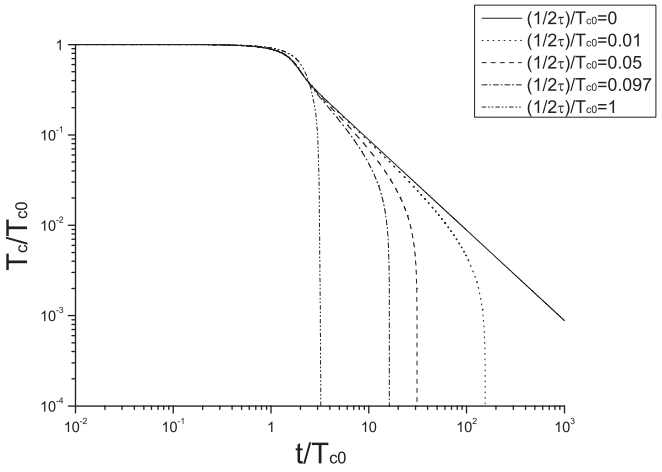

FIG. 9. Graph of T_c/T_{c0} as a function of t/T_{c0}. The clean case $(1/2\tau = 0)$ is presented by the solid line. The impurities are plotted with $(1/2\tau)/T_{c0} = 0.01, 0.05, 0.097, 1$ in dotted, dashed, dashed-dotted, and dashed-dotted-dotted lines, respectively. We see that the impurities enhance the superconducting transition temperature for weak interlayer coupling. On the other hand superconducting critical temperature decreases quickly in the presence of impurities at strong interlayer coupling.

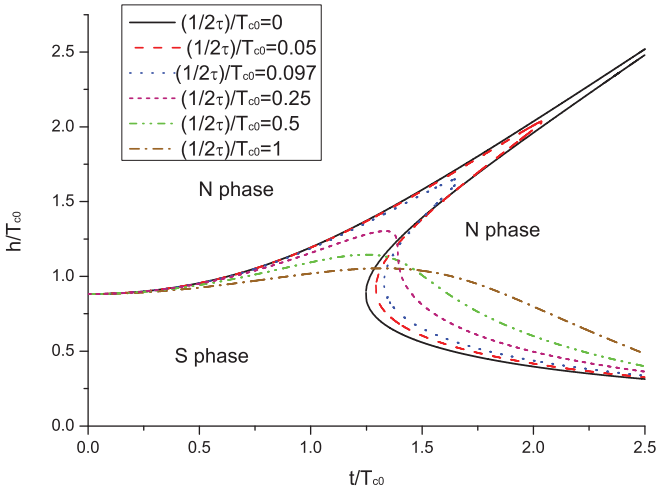

FIG. 10. (Color online) $(h/T_{c0}, t/T_{c0})$ diagram for the S-N bilayer in the clean case $(\tau \to \infty)$ (solid line) and with $(1/2\tau)/T_{c0} = 0.05, 0.097, 1$ in dashed, dotted, dashed-dotted lines, respectively.

decreases slower than in the clean case (see Fig. 9). In this case, the impurities decrease the effective transfer coupling and then the proximity effect.

However, at strong interlayer coupling $t \gg T_{c0}$ and $1/2\tau \ll T_c$, the expression for the anomalous Green's function (18) becomes $f^{+}_{0,0} = \frac{\Delta^*(t^2+2\omega^2)}{2\omega(t^2+\omega^2)}[1 + \frac{t^2(2\omega^2-t^2)}{2\omega(t^2+\omega^2)(t^2+2\omega^2)}(\frac{1}{2\tau})]$ so the critical temperature varies as $\frac{T_c}{T_{c0}} = \frac{\pi e^{-\gamma}}{2}\frac{T_{c0}}{t}(1 - \frac{1}{8}\frac{t}{\tau T_{c0}^2})$. This means that scattering on impurities strongly decreases T_c for high interlayer coupling as seen in Fig. 9. In the regime $t \gg T_{c0}$, the mixing between the superconducting state in the S layer and the normal state in the N layer is very strong. The bilayer draws near the regime $\widetilde{\lambda} \longrightarrow \lambda/2$ where the S-N bilayer can be considered as a single S layer with an effective coupling constant $\widetilde{\lambda} < \lambda$. Note that T_c depends on the impurities contrary to the Anderson theorem prediction which is not surprising because the system is nonuniform.

B. Effect of the impurities on the phase diagram

In this section, we study the influence of the impurities on the (h,T) and (h,t) phase diagram of the S-N bilayer. In the presence of impurities, the modulated phase disappears and h^{FFLO} decreases to h^I.[44,45] When the normal phase is overcooled the critical magnetic field decreases from h^I to h_0.[33] For simplicity in the whole paper, we will focus on the second-order transition critical field of the S-N bilayer, keeping in mind that if the transition is of the first order the calculated field corresponds to the overcooling field and the critical region of superconductivity phase existence may be somewhat larger. Consequently, we study the influence of the impurities in the homogeneous case $(q = 0)$. In this case, the anomalous Green's function is the same as Eq. (18) with the substitution $\omega \longrightarrow \omega + ih$ and can be written as

$$f^{+}_{0,0} = \frac{\Delta_0^*\left[2\left(\omega + ih + \frac{1}{2\tau}\right)^2 + t^2\right]}{\left[2(\omega + ih) + \frac{1}{2\tau}\right]t^2 + 2(\omega + ih)\left(\omega + ih + \frac{1}{2\tau}\right)^2}. \tag{20}$$

1. (h,t) phase diagram at zero temperature

The impurities change the form of the (h,t) phase diagram at $T = 0$ K as shown in Fig. 10. The (h,t) phase diagram has been calculated numerically. The critical interlayer coupling t_c increases with the impurity diffusion potential $1/2\tau$. The maximal values of h_{c1} and h_{c2} decrease with the impurity diffusion potential contrary to h_{c3}. The variations of h_{c1}, h_{c2}, and h_{c3} reveal that the superconducting phase in the S layer is enhanced by the presence of the impurities whereas the field-induced superconducting phase is destroyed by the impurities.

2. (h,T) phase diagram

The (h,T) phase diagram as been calculated numerically. The reentrance phase is strongly influenced by the presence of the impurities as seen in Fig. 11. The maximal critical temperature under which the field-induced phase exists decreases with the impurity scattering potential. Moreover the upper and lower critical fields of the reentrant superconducting phase (h_{c1} and h_{c2}) become closer with the increase of impurity diffusion potential as seen in the previous subsection. In the case $t = 2T_{c0}$, the reentrance phase totally disappears for an impurity diffusion potential $1/2\tau$ above $0.097T_{c0}$. In Fig. 11, the usual superconducting phase is also influenced by the presence of impurities. The critical magnetic field at zero temperature h_{c3} and the critical temperature at zero magnetic field T_c increase with the impurity diffusion potential. The effective interlayer coupling decreases in the presence of impurities and then the usual superconductivity in the S layer is enhanced.

V. EFFECT OF THE IMPURITIES ON THE S-S BILAYER

In this section, we study the S-S bilayer considering the FFLO modulation and the impurities. As predicted in Ref. 22 for ferromagnetic superconductor multilayered systems, a π state may appear in the S-S bilayer under magnetic field. Using the same model as developed in Sec. II, the S-S bilayer is described by the following equations:

$$\begin{pmatrix} \widetilde{\omega} - i\mathbf{v}_F\cdot\mathbf{q} & -i\frac{t}{2} & 0 & i\frac{t}{2} \\ -i\frac{t}{2} & \widetilde{\omega} - i\mathbf{v}_F\cdot\mathbf{q} & i\frac{t}{2} & 0 \\ 0 & i\frac{t}{2} & \widetilde{\omega} - i\mathbf{v}_F\cdot\mathbf{q} & -i\frac{t}{2} \\ i\frac{t}{2} & 0 & -i\frac{t}{2} & \widetilde{\omega} - i\mathbf{v}_F\cdot\mathbf{q} \end{pmatrix} \begin{pmatrix} f^+_{0,0} \\ f^+_{1,0} \\ f^+_{1,1} \\ f^+_{0,1} \end{pmatrix} = \begin{pmatrix} \Delta^*_0 + \frac{\langle f^+_{0,0}(\omega,\mathbf{q})\rangle_\phi}{2\tau} \\ 0 \\ \Delta^*_1 + \frac{\langle f^+_{1,1}(\omega,\mathbf{q})\rangle_\phi}{2\tau} \\ 0 \end{pmatrix},$$

where Δ^*_1 is the superconducting gap in the S layer indexed $j = 1$.

In the π phase, $\Delta^*_0 = -\Delta^*_1$, the solution of the system (21) is

$$f^+_{0,0} = \frac{\Delta^*_0}{2\left(1 - \frac{1}{2\tau}\frac{(\Omega_2+\Omega_1)}{2\Omega_1\Omega_2}\right)}\left(\frac{1}{\omega_1} + \frac{1}{\omega_2}\right)$$

and the averaged solution on the ϕ angle

$$\langle f^+_{0,0}\rangle_\phi = \frac{(\Omega_1+\Omega_2)\,\Delta^*_0}{2\,\Omega_1\Omega_2\left[1 - \frac{1}{2\tau}(\Omega_2+\Omega_1)\right]}.$$

In the clean limit ($\tau \longrightarrow \infty$), at zero temperature, the π superconducting phase appears above the critical magnetic field $h_{\rm low} = t - \Delta_0^2/8t$ and below $h_{\rm up} = t + \Delta_0^2/8t$ in the limit $t \gg \Delta_0$. As predicted in Ref. 21, the modulated FFLO state appears at low temperature and maximizes the critical magnetic field. Hence, with the FFLO state, the critical magnetic fields are $h_{\rm low,up} = t \mp \Delta_0^2/4t$ in the limit $t \gg \Delta_0$. The reentrance superconducting phase is enhanced at low temperature by FFLO modulations. The presence of impurities in the system may destroy the FFLO state and the reentrance phase. The FFLO transition should meet quickly the first-order transition line. Consequently, we will study the influence of the impurities in the homogeneous case where $q = 0$.

A. (h,t) phase diagram

At $T = 0$ K in the π state without FFLO modulation, the self-consistency equation (12) becomes

$$\left[4\left(\frac{1}{2\tau}\right)^2 + \left(2h + \sqrt{\left|-4t^2 + \left(\frac{1}{2\tau}\right)^2\right|}\right)^2\right] \times \left[4\left(\frac{1}{2\tau}\right)^2 + \left(2h - \sqrt{\left|-4t^2 + \left(\frac{1}{2\tau}\right)^2\right|}\right)^2\right] = 16h_0^2. \tag{21}$$

The solutions of Eq. (21) are

$$h^{\rm imp}_{\rm up,low} = \frac{1}{2}\sqrt{\left|-4t^2 + \left(\frac{1}{2\tau}\right)^2\right| - 4\left(\frac{1}{2\tau}\right)^2 \pm 4\sqrt{-\left(\frac{1}{2\tau}\right)^2\left|-4t^2 + \left(\frac{1}{2\tau}\right)^2\right| + h_0^4}},$$

where $h^{\rm imp}_{\rm up,low}$ are the critical magnetic field of the S-S bilayer in the presence of impurities (see Fig. 12). The field-induced superconducting state is destroyed in the presence of impurities and cannot be observed if $h^{\rm imp}_{\rm low} = h^{\rm imp}_{\rm up}$. We define a critical impurity diffusion time $\tau_c = 1/2[2t^2 - (4t^4 - h_0^4)^{1/2}]^{1/2}$ below which the reentrance phase totally disappears. In the case where $t = 2T_{c0}$ and $h_0 = 0.882T_{c0}$, $(\frac{1}{2\tau})_c \simeq 0.194T_{c0}$.

The critical magnetic field in the presence of FFLO modulation is plotted in Fig. 12 in the clean limit. The critical magnetic field in the presence of FFLO modulations is the upper limit of the critical magnetic field.

We can see that $h^{\rm FFLO}_{\rm up}$, the upper critical field in the presence of FFLO modulations, crosses the line $h = \Delta_0$ for $t \simeq 1.25T_{c0}$. This means that the usual superconducting phase is deformed only for $t > 1.25T_{c0}$ at $T = 0$ K. Then the field-induced superconducting phase becomes observable. The field-induced superconducting phase becomes totally observable when $h^{\rm FFLO}_{\rm low}$, the lower critical field in the presence of FFLO modulations, crosses the line $h = \Delta_0$ for $t \simeq 2.1T_{c0}$.

In the uniform case, we would have to consider the first-order transition line. For the S-S bilayer, the first-order transition line is between the second-order and the FFLO

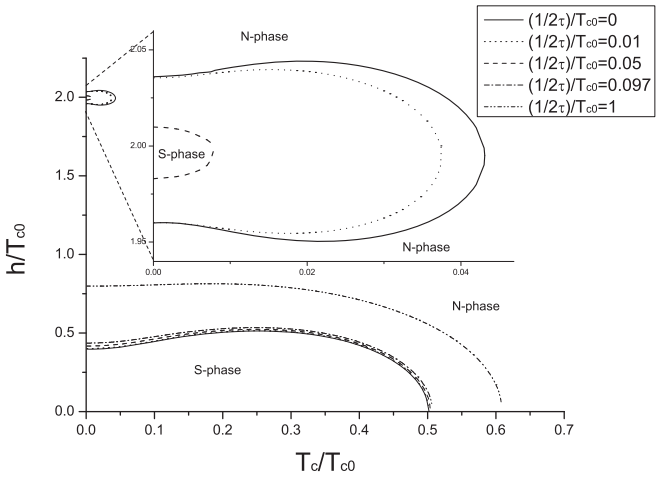

FIG. 11. $(h/T_{c0}, T_c/T_{c0})$phase transition diagram for the S-N bilayer calculated for $t = 2T_{c0}$ with the second-order transition line in the clean case $[(1/2\tau)/T_{c0} = 0]$ (solid line) and with $(1/2\tau)/T_{c0} = 0.01, 0.05, 0.097, 1$ in dotted, dashed, dashed-dotted, dashed-dotted-dotted lines, respectively. The inset presents a zoom of the superconducting reentrance phase around $h \simeq t \simeq 2T_{c0}$.

transition line. The reentrance phase would appear when $h^I_{\rm up}$, the upper critical field for a first-order phase transition, is above $h^I = \Delta_0/\sqrt{2}$ and would be distinguishable if the lower critical field in the case of first-order phase transition is higher than h.

B. (h, T) phase diagram

In the π state, the Cooper pairs are formed by two electrons in different layers. The standard superconducting state is only due to the 0 phase and then is not influenced by the

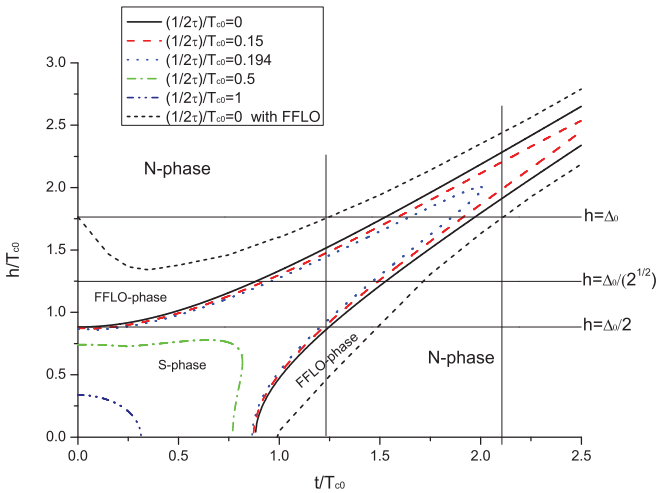

FIG. 12. (Color online) $(h/T_{c0}, t/T_{c0})$ diagram for the S-S bilayer in the clean case $[(1/2\tau)/T_{c0} = 0]$ (solid line) and with $(1/2\tau)/T_{c0} = 0.15, 0.194, 0.5, 1$ in dashed, dotted, dashed-dotted, and dashed-dotted-dotted lines, respectively. The lines $h = \Delta_0/2$, $h = \Delta_0/\sqrt{2}$, and $h = \Delta_0$ present respectively the critical magnetic field for a second-order superconducting phase transition, the critical magnetic field for a first-order phase transition, and the FFLO paramagnetic limit for a single S layer. The close-dashed line is the FFLO paramagnetic limit in the S-S bilayer in the clean limit.

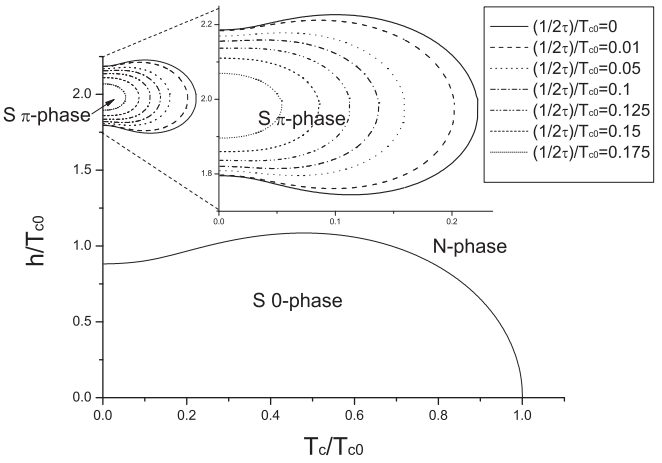

FIG. 13. $(h/T_{c0}, T_c/T_{c0})$ phase transition diagram for the S-S bilayer calculated for $t = 2T_{c0}$ with the second-order transition line in the clean case $[(1/2\tau)/T_{c0} = 0]$ (solid line) and with $(1/2\tau)/T_{c0} = 0.01, 0.05, 0.1, 0.125, 0.15, 0.175$ in dotted, dashed, dashed-dotted, dashed-dotted-dotted, close-dashed, close-dotted lines, respectively. The inset presents a zoom of the superconducting reentrance phase around $h \simeq t \simeq 2T_{c0}$.

impurities as predicted by the Anderson theorem. The lower and upper critical lines merge at field $h = t$ and temperature $T_M = \pi e^{-C} T_{c0}^2/(4t)$ in the limit $t \gg T_{c0}$. The field-induced π superconductivity is confined to temperature lower than T_M.

On the phase diagram, we see that the reentrance decreases as the impurity self-energy is increasing (see Fig. 13). The reentrance phase totally disappears for $\frac{1}{2\tau} \simeq 0.194 T_{c0}$ in the case where $t = 2T_{c0}$. The existence of a first-order transition line in the field-induced phase transition could influence these results. $h^I_{\rm up,low}$ are higher (smaller) than $h_{\rm up,low}$. Consequently, the critical impurity diffusion time τ_c should be higher than in the case of a second-order transition.

VI. CONCLUSION

To conclude, the proximity effect plays a crucial role in the S-N and S-S bilayers. The superconducting critical temperature and the critical magnetic field at zero temperature in the S-N and the S-S bilayers depends directly on the interlayer coupling. We demonstrated that at low temperature, a magnetic-field-induced superconducting phase appears at high in-plane magnetic field in S-N bilayers. This field-induced phase originates from the compensation of Zeeman effect energy splitting by the energy splitting between the bonding and antibonding state electronic levels. This reentrance phase provides the possibility to overcome the classical paramagnetic limit, and the results of our work give hints for engineering layered superconducting material with very high critical fields. Note that the case of S-N bilayers may be relevant to the layered high-T_c superconductors. Indeed, in their crystalline structure often the S and N layers alternate.

In S-S and S-N bilayers, the presence of impurities make the superconducting field-induced phase more difficult to observe. The impurities produce a broadening of the different energy levels over an energy range $1/\tau$ which prevents exact compensation. It is possible to define a critical mean-free path time over

which the reentrance phase cannot survive. In the S-N and S-S bilayers, the critical mean-free path time τ_c only depends on the interlayer coupling. In the S-S bilayer, in the case $t \simeq \Delta_0$, then $\tau_c^{-1} \simeq 0.25\Delta_0$, above which there is no possibility to observe the field-induced phase. From an experimental point of view, it could be possible with molecular beam epitaxy techniques to provide a sufficiently large mean-free path to realize the condition of field-induced phase observation.

Although we have only treated the Zeeman effect as a Cooper pair-breaking effect, we have to discuss the orbital pair-breaking effect. In the case of multilayered system under in-plane magnetic field, the condition for neglecting the orbital effect is given by $tH\xi_0 d/\Phi_0 < \Delta_0$, where ξ_0 is the in-plane coherence length and $\Phi_0 = h/2e$ the superconducting quantum of magnetic flux. In the case $t \simeq \Delta_0$ we obtain that H must be lower than $H_{\rm orb} \simeq \Phi_0/(\xi_0 d)$. At the typical values $d \simeq 10$ Å, $\xi_0 \simeq 100$ Å the corresponding field is extremely large, $H_{\rm orb} \simeq 200$ T, and not restrictive at all, as the maximal currently attainable permanent magnetic field is 60 T. The orbital effect becomes important in layered system in the case $t \gg \Delta_0$ when the Pauli limit may be exceeded many times. However, in Ref. 46 it was demonstrated that the orbital pair breaking in layered superconductors is switched off in the high-field regime and the superconductivity is restored. We may expect that a similar situation would be realized in S-N and S-S bilayers.

ACKNOWLEDGMENTS

The authors would like to thank S. Burdin, V. H. Dao, and A. S. Melnikov for help and useful discussions. This work was supported, in part, by the French ANR SINUS program.

*Also at Institut Universitaire de France, Paris.

[1] L. N. Bulaevskii, Sov. Phys. Usp. **18**, 514 (1975).

[2] N. B. Hannay, T. H. Geballe, B. T. Matthias, K. Andres, P. Schmidt, and D. MacNair, Phys. Rev. Lett. **14**, 225 (1965).

[3] Y. Koike, S. Tanuma, H. Suematsu, and K. Higuchi, Physica B + C **99**, 503 (1980).

[4] E. Jobiliong, H. D. Zhou, J. A. Janik, Y.-J. Jo, L. Balicas, J. S. Brooks, and C. R. Wiebe, Phys. Rev. B **76**, 052511 (2007).

[5] T. E. Weller, M. Ellerby, S. S. Saxena, R. P. Smith, and N. T. Skipper, Nature Phys. **1**, 39 (2005).

[6] A. Buzdin and L. N. Bulaevskii, Sov. Phys. Usp. **27**, 830 (1984); Usp. Fiz. Nauk **144**, 415 (1984).

[7] U. Welp, W. K. Kwok, G. W. Crabtree, K. G. Vandervoort, and J. Z. Liu, Phys. Rev. Lett. **62**, 1908 (1989).

[8] Y. Ive, T. Tamegai, T. Sakakibara, T. Goto, N. Miura, H. Takeya, and H. Takei, Physica C **153-155**, 26 (1988).

[9] M. Oda, Y. Hidaka, M. Suzuki, and T. Murakami, Phys. Rev. B **38**, 252 (1988).

[10] M. Tuominen, A. M. Goldman, Y. Z. Chang, and P. Z. Jiang, Phys. Rev. B **42**, 412 (1990).

[11] J. M. Triscone, M. G. Karkut, L. Antognazza, O. Brunner, and O. Fischer, Phys. Rev. Lett. **63**, 1016 (1989).

[12] J. M. Triscone, O. Fischer, O. Brunner, L. Antognazza, A. D. Kent, and M. G. Karkut, Phys. Rev. Lett. **64**, 804 (1990).

[13] M. Cyrot and D. Pavuna, *Introduction to Superconductivity and High T_c Materials* (World Scientific, Singapore, 1995).

[14] J. R. Cooper, L. Forro, and B. Keszeit, Nature (London) **343**, 444 (1990).

[15] S. Martin, A. T. Fiory, R. M. Fleming, L. F. Schneemeyer, and J. V. Waszczak, Phys. Rev. Lett. **60**, 2194 (1988).

[16] Y. Hidaka, Y. Enomoto, M. Suzuki, M. Oda, and T. Murakami, Jpn. J. Appl. Phys. **26**, L377 (1987).

[17] T. Nachtrab, Ch. Bernhard, Ch. Lin, D. Koelle, and R. Kleiner, C. R. Phys. **7**, 68 (2006).

[18] M. Tinkham, *Introduction to Superconductivity* (Dover Publications, 1996).

[19] V. L. Ginzburg, Zh. Eksp. Teor. Fiz. **23**, 236 (1952).

[20] W. E. Lawrence and S. Doniach, in *Proceedings of the Twelfth International Conference on Low Temperature Physics, Kyoto, 1970*, edited by E. Kanda (Keigaku, Tokyo, 1970), p. 361.

[21] S. Tollis, J. Cayssol, and A. I. Buzdin, Phys. Rev. B **73**, 174519 (2006).

[22] A. V. Andreev, A. I. Buzdin, and R. M. Osgood III, Phys. Rev. B **43**, 10124 (1991).

[23] S. Tollis, M. Daumens, and A. I. Buzdin, Phys. Rev. B **71**, 024510 (2005).

[24] M. Houzet and A. Buzdin, Europhys. Lett. **58**, 596 (2002).

[25] V. Prokic, A. I. Buzdin, and L. Dobrosavljevic-Grujic, Phys. Rev. B **59**, 587 (1999).

[26] A. I. Buzdin, S. Tollis, and J. Cayssol, Phys. Rev. Lett. **95**, 167003 (2005).

[27] A. I. Buzdin, S. Tollis, and J. Cayssol, Physica C **460-462**, 1028 (2007).

[28] M. L. Kulic and U. Hofmann, Solid State Commun. **77**, 717 (1991).

[29] A. I. Larkin and Y. N. Ovchinnikov, Sov. Phys. JETP **20**, 762 (1965).

[30] P. Fulde and R. A. Ferrell, Phys. Rev. **135**, A550 (1964).

[31] L. N. Bulaevskii and M. V. Zyskin, Phys. Rev. B **42**, 10230 (1990).

[32] P. G. de Gennes, *Superconductivity of Metals and Alloys* (Westview Press, 1999).

[33] D. Saint-James, G. Sarma, and E. J. Thomas, *Type II Superconductivity* (Pergamon, Oxford, 1969).

[34] A. Bianchi, R. Movshovich, C. Capan, P. G. Pagliuso, and J. L. Sarrao, Phys. Rev. Lett. **91**, 187004 (2003).

[35] C. Capan, A. Bianchi, R. Movshovich, A. D. Christianson, A. Malinowski, M. F. Hundley, A. Lacerda, P. G. Pagliuso, and J. L. Sarrao, Phys. Rev. B. **70**, 134513 (2004).

[36] S. Uji, H. Shinagawa, T. Terashima, T. Yakabe, Y. Terai, M. Tokumoto, A. Kobayashi, H. Tanaka, and H. Kobayashi, Nature (London) **410**, 908 (2001).

[37] B. S. Chandrasekhar, Appl. Phys. Lett. **1**, 7 (1962).

[38] A. M. Clogston, Phys. Rev. Lett. **9**, 266 (1962).

[39] L. N. Bulaevskii, Sov. Phys. JETP **37**, 1133 (1973).

[40] A. I. Buzdin and V. V. Tugushev, Sov. Phys. JETP **58**, 428 (1983).

[41] A. A. Abrikosov, L. P. Gorkov, and I. Dzyaloshinsky, *Methods of Quantum Field Theory in Statistical Physics* (Prentice Hall, 1963).

[42] G. Eilenberger, Z. Phys. **190**, 142 (1966).

[43] N. Kopnin, *Theory of Nonequilibrium Superconductivity* (Clarendon Press, Oxford, 2001).

[44] L. G. Aslamazov, Sov. Phys. JETP **28**, 773 (1969).

[45] L. N. Bulaevskii and A. A. Guseinov, Sov. J. Low Temp. Phys. **2**, 140 (1976).

[46] A. G. Lebed and K. Yamaji, Phys. Rev. Lett. **80**, 2697 (1998).